Lab on a Chip

Dynamic Article Links

Cite this: *Lab Chip*, 2012, **12**, 5225–5230

www.rsc.org/loc

PAPER

Blood plasma separation in a long two-phase plug flowing through disposable tubing†

Meng Sun, Zeina S. Khan and Siva A. Vanapalli*

Received 11th May 2012, Accepted 7th October 2012
DOI: 10.1039/c2lc40544j

We report a simple technique to separate plasma from blood in a flowing immiscible plug. We investigate the effect of various control parameters such as blood dilution, injection flow rate, observation time and fluid properties on plasma separation. We find that the technique works best for diluted blood samples at low plug velocities and long observation times. We postulate that the main mechanism responsible for efficient separation is the sedimentation of blood cells in the plug and their subsequent collection by the moving plug causing a significant accumulation of cells at the rear of the plug. We discuss the time scales determining the sedimentation, advection and collection of a blood cell in the immiscible plug and propose a phase diagram that is able to predict the operating space for effective plasma separation. We demonstrate that the technique allows for the extraction of more than 60% of the plasma by volume from 1 μL of diluted blood. We show the practical significance of this method by compartmentalizing the separated plasma into discrete microfluidic droplets and detecting cholesterol. This technique features low consumption of blood (nL-scale) and low shear rate (~ 1 s^{-1}). It is inexpensive, easy to use, and has the potential to be developed as an efficient point-of-care device for blood diagnostics in resource-poor environments. More advanced applications could also be envisioned by integrating our plasma separation method into existing microfluidic drop manipulation techniques.

I. Introduction

Blood is a biological fluid that provides a wealth of information on the state of human health. For this reason, blood tests are necessary for nearly every clinical diagnosis. The two main constituents of blood are plasma and red blood cells (RBCs). Plasma comprises ~55% of blood and contains many biomarkers including cholesterol, proteins and circulating DNA which are frequently used for the clinical diagnosis of diseases ranging from cardiovascular disorders to cancer.[1,2] The first step in detecting the biomarkers usually requires the removal of blood cells from the plasma since the cells could interfere with the accuracy of the tests. The traditional method for separating plasma from blood utilizes a bench-top centrifuge. Blood cells precipitate to the bottom of a tube, while plasma is the supernatant and is decanted from the top after centrifugation. This method consumes milliliters of blood and relies not only on the availability of equipment, but also on access to a reliable source of electricity.

Recently, microfluidic techniques have attracted great interest for isolating plasma from other cellular components in miniaturized devices.[3–5] The benefits of utilizing these approaches include low consumption of samples or reagents, improved sensitivity and faster diagnosis. On the microscale, the delamination of plasma and blood cells can be driven by gravitational[6–8] or other external fields such as on-chip centrifugation,[9] dielectrophoresis,[10] acoustophoresis[11] and magnetophoresis.[12] Plasma can also be separated from blood *via* filtration through packed beads,[13] membranes,[14] pillars[15] or weirs[16] fabricated in a microfluidic channel while the blood cells are retained due to their size. In addition, blood flow in microchannels induces the Zweifach–Fung effect[17] or inertial lift forces,[18,19] which leads to the separation of plasma from blood cells which are then directed to different branches or outlets. However, most microfluidic approaches make use of microfabrication techniques and have complicated channel networks which require intensive training to fabricate and operate. Moreover, because of the continuous flow of blood through the devices, significant dead volumes may result based on the amount of time needed to stabilize the flow. A portable, easy-to-use and inexpensive instrument for the on-site analysis of plasma constituents would be well suited to point-of-care (POC) testing especially in resource-poor areas.[20] For example, an egg-beater based plasma separation device was recently reported, which required the use of 100 μL of blood and 8 min of hand-centrifugation.[21]

Unlike prior microfluidic blood plasma separation devices, which were based on single-phase flow, here we report a simple

Department of Chemical Engineering, Texas Tech University, Lubbock, TX, 79409-3121, USA. Fax: +1-806-742-3552; Tel: +1-806-742-1757

† Electronic supplementary information (ESI) available: experimental section and two movies showing the separation of plasma in a flowing blood plug. See DOI: 10.1039/c2lc40544j

technique to separate plasma from blood using long two-phase plugs. This method is motivated by the observations made during our recent study, in which we tried to encapsulate leukemia cells and particles in static droplet arrays by injecting long immiscible plugs into a chip using a cartridge.[22] We observed that larger particles, such as leukemia cells, would accumulate at the rear of the immiscible plug (unpublished data). Recently, Kurup *et al.*[23] have reported a similar collection phenomenon using spherical particles and argue that the sedimentation of dense particles coupled with particle transport due to fluid circulation are responsible for particle accumulation in the plug. Here we exploit this phenomenon and show that when a long immiscible plug of blood flows through disposable tubing surrounded by an oil carrier phase, blood cells in the plug accumulate in the back of the moving plug while plasma is located in the front and isolated from the cells (see Fig. 1). For a given size of tubing, we investigate the factors influencing the efficiency of plasma separation. Subsequently we discuss the underlying mechanism that is well corroborated by experimental data. We also demonstrate that the plasma portion of the plug in the tubing can be effectively utilized by connecting it to microfluidic devices, separating it into drops, and combining it with chemical reagents to perform a colorimetric cholesterol detection assay.

II. Control parameters influencing plasma separation

In a typical experiment, we aspirated 1 μL of blood into an oil-filled cartridge, followed by a certain volume of oil to sandwich the blood plug in carrier oil. Depending on the flow rate and blood dilution, the plasma can separate from the blood cells in both the aspiration and infusion steps as long as there is oil behind the plug pushing it through the tubing. As shown in Fig. 1 and Movies S1 and S2, ESI†, cells accumulate in the rear of blood plug.

To investigate the influence of blood hematocrit on the efficiency of plasma separation, we diluted whole blood to five different concentrations with phosphate-buffered saline (PBS) and prepared cartridges containing 1 μL of blood flanked by 1 μL of oil on either side. The cartridges were connected to a microchannel to enable clear visualization of the plasma separation. Fig. 2 shows top-view snapshots of the plugs in a microchannel after they have displaced 3 μL of oil at a flow rate of 0.5 μL min^{-1}. In Fig. 2, the shade of gray reflects the density of the cells at different locations in the plug. A dark shade indicates a high cell density. Using this grayscale analysis, we quantify the efficiency of plasma separation as the fraction of the plug occupied by the cell-free fluid. When the dilution increases from 5 to 20 fold, the portions of the plasma isolated in the diluted blood are 40%, 63% and 72%. For non-diluted whole blood and 2-fold diluted blood, the plasma failed to fully separate from the cells at a flow rate of 0.5 μL min^{-1}. We note that all the images in Fig. 2 were taken at an observation time, t_{obs} = 360 s. Here the observation time is defined as the time period from when the plug starts pushing the oil in front of it until a known volume of oil is displaced. For example in Fig. 2, the displaced oil volume is 3 μL and the flow rate is 0.5 μL min^{-1}, therefore t_{obs} is 360 s.

To determine the effect of the injection flow rate on the quality of plasma separation, we used a 10-fold diluted blood plug. Cartridges were prepared in a manner similar to that used to study the effect of hematocrit and the observation time t_{obs} was maintained at 360 s. As shown in Fig. 3, higher separation efficiencies are achieved for lower volumetric flow rates, which decrease from 77% at 0.2 μL min^{-1} to 43% at 1.0 μL min^{-1}. At 2.0 μL min^{-1}, it is difficult to define the interface between the plasma and the cells since a few cells are still present in the front part of plug, while at 4.0 μL min^{-1}, there is very little separation of plasma in the blood plug.

It is possible that higher flow rates appear to result in less efficient separation because of the short observation times that were used. We therefore probed the effect of varying the observation time at a fixed flow rate. To vary t_{obs}, we controlled the volume of oil (0.5, 1, 2 and 4 μL) present in front of a fixed volume (1 μL) of a 10-fold diluted blood plug. The cartridge was inserted into the microfluidic channel for visualization and the fluids were infused at a rate of 0.5 μL min^{-1}. We recorded movies of the traveling plug at a fixed top view location. To quantify the separation efficiency, we computed the mean grayscale value (by averaging over a line of pixels perpendicular to the direction of the plug flow) at a fixed location downstream of the cartridge–microchannel intersection for every image in the movie. The mean grayscale values are shown in Fig. 4 against the

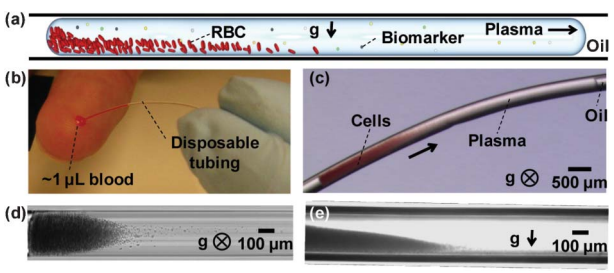

Fig. 1 Blood plasma separation in a plug. (a) Schematic diagram showing the separation of blood cells in a moving plug surrounded by oil. (b) ~1 μL of blood is taken from a finger prick and aspirated into disposable tubing. (c) Demonstration of plasma and blood cell separation in a 200 nL plug (20 nL whole blood). Close-up of the separation interface between the plasma and the cells: (d) top view; (e) side view. The arrows indicate the direction of flow. "g" indicates the direction of gravity.

Fig. 2 Top-view images of plasma separation from blood cells for different concentrations of whole blood. (a) Non-diluted whole blood. (b–e) Blood diluted 2, 5, 10 and 20 times by PBS. The flow rate is 0.5 μL min^{-1}.

Fig. 3 The influence of flow rate on the separation efficiency: plasma isolated in a 10-fold diluted blood plug at flow rate of (a) 0.2, (b) 0.5, (c) 1.0, (d) 2.0, and (e) 4.0 μL min^{-1}. These images are of the top view.

elapsed time since the plug has entered the field of view; this constitutes a spatial measurement of grayscale along the length of the plug, where the position along the length of the plug corresponding to each time point is simply the product of the plug velocity and the elapsed time. We found that for t_{obs} = 60 s, the amount of accumulated cells at the back of the plug was low. We did not observe a clear interface between the plasma and the cells in the plug for a short observation time (as indicated by the gradually decreasing grayscale values at short times in Fig. 4a). In contrast, at longer observation times of 120, 240 and 480 s (Fig. 4b–d), we found a significant reduction in the grayscale value indicating a clear separation between the cells and the plasma. The time for the separation to be fully achieved was 120–240 s and we didn't observe a significant enhancement of the separation efficiency ($\sim$66% for Fig. 4c, d) when the observation time increased from 240 s to 480 s.

Thus, we have shown that the efficient separation of the plasma of cells can be achieved by infusing 1 μL of 5–20-fold diluted blood plugs behind 1–2 μL of an oil carrier at volumetric flow rates of 0.2–1.0 μL min^{-1}. The repeatability of the separation efficiency was also found to be excellent. In five independent experiments conducted at the same flow rate (0.5 μL min^{-1}) and observation time t_{obs} = 360 s, we have observed that the separation efficiency is 64.01%, 62.91%, 63.16%, 63.07%, and 64.04% of plasma (v/v) isolated from 10-fold diluted blood in a 1 μL plug. The computed relative standard deviation from this data set is <0.6%.

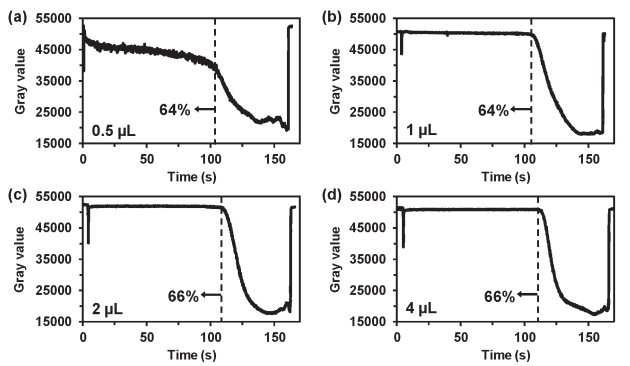

Fig. 4 The effect of increasing the observation time of a blood plug on the separation efficiency: plasma isolated in a 10-fold diluted blood plug infused at a rate of 0.5 μL min^{-1} behind (a) 0.5, (b) 1, (c) 2, and (d) 4 μL of oil.

III. Description of the plasma separation mechanism

Our observations described above indicate that blood cells collect at the back of long plugs resulting in the separation of the plasma. In the plug, the blood cells experience a number of forces including viscous fluid forces, gravitational forces and inter-particle forces that could lead to aggregation. In addition to these forces, the kinematics of the flow in the plug could also affect the distribution of blood cells in the plug. Indeed, Kurup *et al.*[23] suggest that for the case of microspheres and short plugs ($L/W < 10$, here L and W are the plug length and width respectively), sedimentation, aggregation and fluid circulation can play a role in the separation properties. In our experiments with long plugs ($L/W > 100$), we postulate that the main mechanism responsible for efficient separation is the sedimentation of the cells to the bottom of the plug due to gravity, and if sufficient observation time is allowed, the moving plug collects the sedimented cells at the rear of the plug. Below, we estimate the time scales which govern this mechanism, and provide experimental data to support our interpretation of the relevant time scales which govern this process.

(i) Sedimentation time (t_s)

At the dilute limit, we estimate that the time required for a single red blood cell to sediment to the lower half of the tube is given by $t_s = R_p/V_s$, where $V_s = (2a^2\Delta\rho g)/(9\mu_P)$ is the sedimentation velocity, determined by equating the gravitational force acting on a sphere ($F_G = (4/3)\pi a^3\Delta\rho g$) with the drag force acting on it due to the presence of the liquid ($F_D = 6\pi\mu_P a V_s$).[24] Here R_p is the radius of the tube, a is the particle radius ($\sim$3.5 μm for a red blood cell,)[21] $\Delta\rho$ is the difference in the density between the cell and liquid medium ($\sim$97 kg m^{-3} for a red blood cell),[21] g is the acceleration due to gravity and μ_P is the viscosity of the fluid in the plug (2.8–1.5 mPa s for blood diluted 5–20 times with PBS).[25] This situation is illustrated in Fig. 5a.

To verify whether sedimentation plays a role in particle collection, we conducted experiments using polystyrene microparticles (a = 5 μm, ρ = 1050 kg m^{-3}) where the density of the fluid was varied by diluting it with deuterium oxide (D_2O, ρ = 1105 kg m^{-3}). As shown in side view images of the back of the plug in Fig. 6, only when there is a density difference between the particles and fluid do we find appreciable separation of the particles at the rear of the plug. We also observe that the collection zone is at the bottom of the plug when the particles are denser than the liquid, and at the top when the particles are less dense than the liquid, thereby confirming the role of sedimentation in our observations.

(ii) Advection time (t_{adv})

Particle transport due to the flow field in the plug could also affect the separation efficiency, since the fluid flow can advect cells to either the front or rear of the plug, shown schematically in Fig. 5b. This transport depends on the nature of the flow field and the particle's position in the flow field. We therefore quantified the flow field in long plugs by seeding 2 μm microparticles in PBS and tracking their positions in the flow

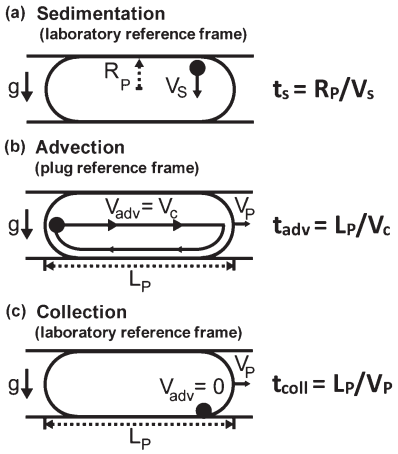

Fig. 5 Illustration of the timescales for a spherical particle to be collected in the back of a flowing plug. (a) Sedimentation occurs when the force of gravity acting on the particle exceeds the drag force, and the particle sediments with a velocity V_s. (b) Particle advection can occur in an axisymmetric parabolic flow field; we have illustrated the particle being advected away from the accumulation zone with the fastest velocity along the centerline. (c) Particle collection can occur if the particle has sedimented to the edge of the plug and is collected at the back.

field. Velocities were determined by differentiating the trajectories in time. Fig. S1, ESI,† shows the experimentally derived velocity vector map in the reference frame of the plug. We find that there is a single toroidal flow in the plug, with the bulk of the fluid in the center of the plug moving in the same direction as the plug, and a small amount at the edges moving in the opposite direction. Since the bulk of the fluid flow field approximates a Poiseuille axisymmetric parabolic velocity profile,[23,26] the minimum advection time would be along the centerline. The centerline velocity (V_c) from our particle tracking experiments (see Fig. S1, ESI†) and modeling by Hodges *et al.*[26] indicates that it is of the order of the mean plug velocity, V_p. Therefore we estimate $t_{adv} = L_p/V_c = L_p/V_p$, where L_p is the plug length. We have selected the minimum advection time occurring at the center of the plug since this quantity relative to the sedimentation time t_s should indicate if the strength of the flow field affects the particle's ability to sediment.

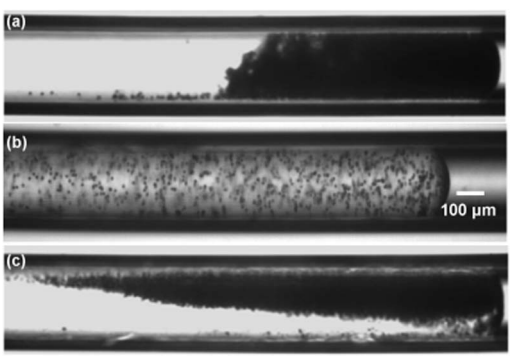

Fig. 6 The influence of a density mismatch between the particles and the fluid on particle sedimentation and collection. (a) Polystyrene beads in PBS, $\Delta\rho = 50$ kg m^{-3}, $t_s = 37$ s. (b) Polystyrene beads in a 1 : 1 mixture with D_2O, $\Delta\rho = -3.5$ kg m^{-3}, $t_s = 533$ s. (c) Polystyrene beads in a 1 : 2 mixture with D_2O, $\Delta\rho = -21.3$ kg m^{-3}, $t_s = 87$ s. For these experiments $t_{obs} = 120$ s, $t_{coll} = 96$ s, $t_{adv} = 96$ s and the volumetric flow rate $Q = 0.5$ μL min^{-1}.

(iii) Collection time (t_{coll})

According to our postulated mechanism, the sedimented blood cells need to be scooped by the moving plug if they are to form a collection zone at the back of the plug, therefore it is important to determine the time for this collection of cells. As shown schematically in Fig. 5c, the limiting collection time can be estimated as $t_{coll} = L_p/V_p$. Here we have assumed that the cell is located at the lower boundary of the plug, where its velocity is zero in the laboratory frame of reference.

In addition to the three time scales discussed so far, the results of Fig. 4 indicate that the observation time also affects the separation efficiency. Considering all of these competing time scales, it is expected that if $t_s/t_{adv} < 1$, then a collection of cells will be observed in the bottom of the plug in the side view experiments given an appropriate t_{obs}. If however, $t_s/t_{adv} > 1$, then no sediment will be observed in the side view experiments regardless of the t_{obs} chosen. Similarly, if a particle were to sediment in a regime where $t_s/t_{adv} < 1$, and if $t_{coll}/t_{obs} < 1$ then no cells would be observed at the front of the plug in experiment. However, if $t_s/t_{adv} < 1$ and $t_{coll}/t_{obs} > 1$, a sediment would be observed at the front of the plug in the experiment. We note that since the moving plug can pass through the field of view over the course of several minutes (typically 1–5 min), we take t_{obs} to be the shortest possible observation time (*i.e.* the time period elapsed from when the plug motion begins until the plug appears in the field of view).

We have performed numerous side view plug imaging experiments to check the validity of these arguments by varying several of the timescales. We have increased the viscosity of the diluted blood samples by adding glycerol to PBS while keeping the plug velocity and the observation time fixed; this results in a systematic increase of t_s while $t_{adv} = 240$ s, $t_{coll} = 240$ s and $t_{obs} = 300$ s are held fixed, shown in Fig. 7a–d. In Fig. 7a, where $t_s/t_{adv} > 1$, no sedimentation is observed. In Fig. 7b, where $t_s/t_{adv} = 0.65$ and $t_{coll}/t_{obs} = 0.8$ (*i.e.* both ratios are smaller than 1), we observe that sediment is present in the front of the plug. However, as this plug passes through the field of view, we also observe an accumulation zone at the rear of the plug which means that this collection of sediment occurs at a longer observation time. Finally, in Fig. 7c and d, where $t_s/t_{adv} < 1$ and $t_{coll}/t_{obs} < 1$, we observe that the front is devoid of cells, and

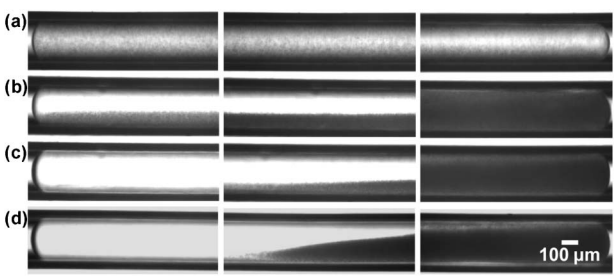

Fig. 7 The influence of increasing the fluid viscosity on 5-fold diluted blood. (a) $\mu_P = 10.6$ mPa s, $t_s = 417$ s. (b) $\mu_P = 4$ mPa s, $t_s = 157$ s. (c) $\mu_P = 3$ mPa s, $t_s = 120$ s. (d) $\mu_P = 2.8$ mPa s, $t_s = 110$ s. For all experiments, $t_{coll} = 240$ s, $t_{adv} = 240$ s, $t_{obs} = 300$ s, and $Q = 0.2$ μL min^{-1}.

the sediment has been collected at the back of the plug when it arrives in the field of view. Additionally, viscosity influences the cell collection effect, as suggested by the steepness of the plasma/cells interface in Fig. 7c, d, resulting in an increase in the separation efficiency from 51% to 79%.

We have also varied the velocity of a diluted blood plug while keeping t_s fixed, which is equivalent to varying t_{adv}, t_{coll} and t_{obs}, as shown in Fig. S2, ESI.† The plasma is separated from the blood cells in the front of plugs at the low flow rates of 0.1 and 0.2 μL min^{-1} (Fig. S2e and f, ESI†). We also observe that as t_s/t_{adv} increases above 1, and simultaneously, as t_{coll}/t_{obs} increases above 1, the blood cells undergo a transition from being sedimented to being suspended (Fig. S2d–a, ESI†).

In Fig. 8, based on the two parameters t_s/t_{adv} and t_{coll}/t_{obs}, we summarize the data from all of our experiments including Fig. 2–4, 6, and 7, and Fig. S2 and S3, ESI† (a detailed tabulation of the data is provided in Table S1 in the ESI†). The zone demarcated by $t_s/t_{adv} < 1$ and $t_{coll}/t_{obs} < 1$ is where both the sedimentation and accumulation of particles at the tail of the plug is expected to occur. Indeed, all of the experimental data in which we observed sedimentation and separation lie in this zone. Likewise for $t_s/t_{adv} > 1$, we expect neither sedimentation nor separation to occur, and our observations are in good agreement with this prediction. Thus, our model based on competing time scales predicts these two limits of particle behavior in long plugs well. However, it is unable to explain the transitional behaviors where the sedimentation of blood cells occurs but no separation occurs at the front of the plug. This may be due to the reduced ability of the blood cells to be transported to the rear of the plug because of the presence of a highly viscous sediment layer. Nevertheless, the two parameters presented in Fig. 8 can be used to design and optimize blood plasma separation. For example, the analysis presented above predicts that non-diluted whole blood can take

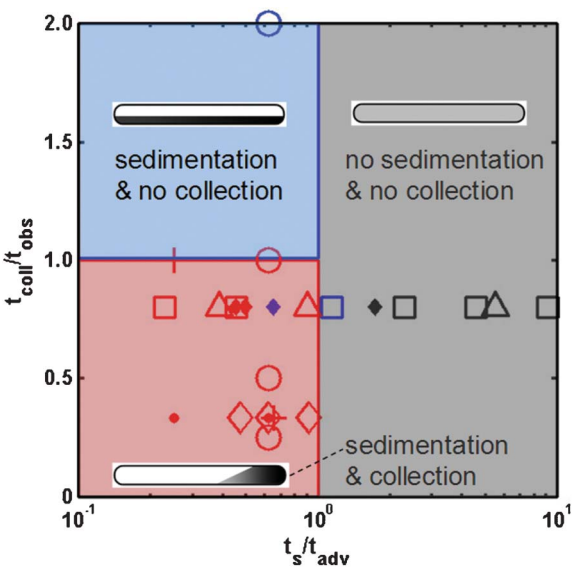

Fig. 8 Diagram showing the sedimentation and collection behavior of the particles. The colored symbols correspond to our observation of sedimentation and collection (red), sedimentation alone (blue), and no sedimentation or collection (black), and the background colors of the different "zones" demarcate our expectation of what will occur. See text for details.

13–65 min to separate because of its high viscosity at low shear rates (20–100 mPa s).[27] When we conducted an experiment with non-diluted whole blood, we found that it took ~40 min for plasma separation to occur (see Fig. S3b, ESI†), consistent with the range estimated by our simple model.

IV. Coupling plasma separation to droplet-based microfluidics for biomarker detection

The simplicity and robustness of this technique to separate plasma in diluted blood samples offers unique opportunities for drop-based technologies. For example, even though significant advances have been made in droplet-based microfluidics, current studies[28,29] have not been able to integrate blood plasma separation into drop-production devices and rely on off-chip separation. However, as shown in Fig. 9a and b, it is straightforward to split the plasma portion of the blood plug into discrete droplets with a T-junction. We have produced 86 clear plasma droplets and 41 droplets containing blood cells as shown. The ratio of isolated plasma-filled drops to blood-cell containing drops is close to the volume fraction of isolated plasma in the flowing blood plug (~66%). Interestingly, as shown in Fig. 9b, this method also delivers the capability to produce droplets with a gradually varying cell density, which could be a useful tool for cell-based assays.

We note that although single-phase devices (based on, for example, inertial migration[18,19]) can be used to extract plasma and coupled to drop generation devices in a modular fashion, challenges might be present because pressure fluctuations induced by confined drop production could couple in an uncontrolled way to the hydrodynamic pressure distribution needed for skimming plasma from the single-phase device. Another concern during plasma separation in single-phase microfluidic devices is the possibility of shear-induced cell lysis due to the high shear rates (~1000 s^{-1}). In our method, because the shear rates are very low (~1 s^{-1}), the plasma is expected to be essentially cell lysis-free in the plug.

Finally, to demonstrate the applicability of the technique to detect simple biomarkers such as cholesterol, which is relevant for POC applications, we implemented a colorimetric assay using Amplex Red as a cholesterol indicator. The clear isolated plasma channel merged with a channel containing colorless Amplex Red in the microfluidic device upstream of the T-junction where drops are produced (see Fig. 9c). This combined stream was then fragmented by oil to produce a train of pink droplets, where the color is due to the reaction of horseradish peroxidase (HRP) and Amplex Red in the presence of hydrogen peroxide (H_2O_2), which is a product of cholesterol and cholesterol oxidase present in the plasma.

The ability to detect cholesterol indicates that even though diluted blood was used in the assay, our method is relevant for certain diagnostic applications. Other diagnostic assays may require non-diluted whole blood, in which case our technique will require a long sample preparation time (~40 min), which makes our approach best suited for assays that can accommodate dilution. However, the ability of our method to encapsulate plasma and reagent directly into droplet-based microreactors could confine the diffusible species by eliminating the dispersion of biomolecules that is typically present in single-phase plasma

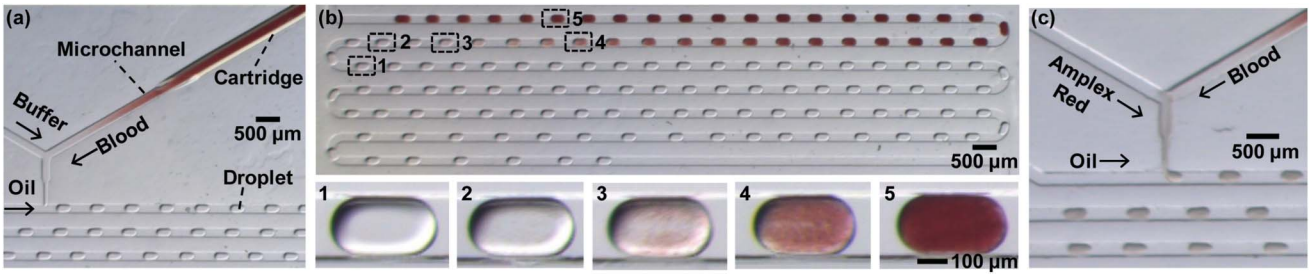

Fig. 9 Isolated blood plasma and cells split into individual droplets. (a) The introduction of a blood plug into a microchannel and the fragmentation of the plug into droplets. (b) A droplet array shows the droplets containing clear plasma and a density gradient of the cells indexed with the numbers 1–5 (see close-up images). (c) Plasma mixing with Amplex Red to form a colorimetric assay where the pink droplets produced downstream indicate the presence of cholesterol in the plasma.

separation and analysis systems, thus enhancing the sensitivity of the assays and reducing the detection time.[30] Potential applications in this field are drop-based digital PCR on circulating tumor DNA for cancer diagnostics;[31,32] and the detection of protein biomarkers in plasma relevant for cardiovascular diseases.[33,34]

V. Conclusions

In conclusion, we have demonstrated a very simple technique to isolate plasma from blood in a long flowing immiscible plug. With this technique more than 60% of the plasma by volume can be extracted from 1 μL of diluted blood and less than 200 nL of non-diluted whole blood is required. It takes ~1 min to load the blood sample and carrier fluid and 2–4 min for fractionation to occur. Without requiring the fabrication of microfluidic chips with complicated channel networks, all of the operations can be simply accomplished using inexpensive disposable tubing. These features meet the requirements for a POC device, where an appropriate driving module for the fluids (*e.g.* gravity-driven flow) needs to be integrated. We also discuss the underlying mechanism for plasma separation in long plugs, which is well supported by experimental data. This mechanistic understanding should enable the rational design and optimization of more advanced drop-based platforms where discrete plasma droplets can be merged with other reagent-loaded drops for sensitive biomolecule analysis.

Acknowledgements

We acknowledge the National Science Foundation (CAREER: 1150836) and Cancer Prevention and Research Institute of Texas (CPRIT: RP100756) for partially supporting this work.

References

1 K. Jung, M. Fleischhacker and A. Rabien, *Clin. Chim. Acta*, 2010, **411**, 1611.
2 Z. H. Nie, F. Deiss, X. Y. Liu, O. Akbulut and G. M. Whitesides, *Lab Chip*, 2010, **10**, 3163.
3 H. W. Hou, A. A. S. Bhagat, W. C. Lee, S. Huang, J. Han and C. T. Lim, *Micromachines*, 2011, **2**, 319.
4 M. Toner and D. Irimia, *Annu. Rev. Biomed. Eng.*, 2005, **7**, 77.
5 M. Radisic, R. K. Iyer and S. K. Murthy, *Int. J. Nanomed.*, 2006, **1**, 3.
6 T. Tachi, N. Kaji, M. Tokeshi and Y. Baba, *Anal. Chem.*, 2009, **81**, 3194.
7 I. K. Dimov, L. Basabe-Desmonts, J. L. Garcia-Cordero, B. M. Ross, A. J. Ricco and L. P. Lee, *Lab Chip*, 2011, **11**, 845.
8 X. B. Zhang, Z. Q. Wu, K. Wang, J. Zhu, J. J. Xu, X. H. Xia and H. Y. Chen, *Anal. Chem.*, 2012, **84**, 3780.
9 S. Haeberle, T. Brenner, R. Zengerle and J. Ducree, *Lab Chip*, 2006, **6**, 776.
10 Y. Nakashima, S. Hata and T. Yasuda, *Sens. Actuators, B*, 2010, **145**, 561.
11 A. Lenshof, A. Ahmad-Tajudin, K. Jaras, A. M. Sward-Nilsson, L. Aberg, G. Marko-Varga, J. Malm, H. Lilja and T. Laurell, *Anal. Chem.*, 2009, **81**, 6030.
12 E. P. Furlani, *J. Phys. D: Appl. Phys.*, 2007, **40**, 1313.
13 J. S. Shim, A. W. Browne and C. H. Ahn, *Biomed. Microdevices*, 2010, **12**, 949.
14 T. A. Crowley and V. Pizziconi, *Lab Chip*, 2005, **5**, 922.
15 J. A. Davis, D. W. Inglis, K. J. Morton, D. A. Lawrence, L. R. Huang, S. Y. Chou, J. C. Sturm and R. H. Austin, *Proc. Natl. Acad. Sci. U. S. A.*, 2006, **103**, 14779.
16 V. VanDelinder and A. Groisman, *Anal. Chem.*, 2006, **78**, 3765.
17 S. Yang, A. Undar and J. D. Zahn, *Lab Chip*, 2006, **6**, 871.
18 A. J. Mach and D. Di Carlo, *Biotechnol. Bioeng.*, 2010, **107**, 302.
19 M. Faivre, M. Abkarian, K. Bickraj and H. A. Stone, *Biorheology*, 2006, **43**, 147.
20 V. Gubala, L. F. Harris, A. J. Ricco, M. X. Tan and D. E. Williams, *Anal. Chem.*, 2012, **84**, 487.
21 A. P. Wong, M. Gupta, S. S. Shevkoplyas and G. M. Whitesides, *Lab Chip*, 2008, **8**, 2032.
22 M. Sun, S. S. Bithi and S. A. Vanapalli, *Lab Chip*, 2011, **11**, 3949.
23 G. K. Kurup and A. S. Basu, *Biomicrofluidics*, 2012, **6**, 022008.
24 W. B. Russel, D. A. Saville and W. R. Schowalter, *Colloidal Dispersions*, Cambridge University Press, Cambridge, UK, 1989, p.394.
25 Blood viscosity, http://en.wikipedia.org/wiki/Blood_viscosity, *from Wikipedia, the free encyclopedia*, 10 July, 2012.
26 S. R. Hodges, O. E. Jensen and J. M. Rallison, *J. Fluid Mech.*, 2004, **501**, 279.
27 S. Chien, *Science*, 1970, **108**, 977.
28 M. J. Jebrail, H. Yang, J. M. Mudrik, N. M. Lafreniere, C. McRoberts, O. Y. Al-Dirbashi, L. Fisher, P. Chakraborty and A. R. Wheeler, *Lab Chip*, 2011, **11**, 3218.
29 H. Song, H. W. Li, M. S. Munson, T. G. Van Ha and R. F. Ismagilov, *Anal. Chem.*, 2006, **78**, 4839.
30 M. E. Vincent, W. S. Liu, E. B. Haney and R. F. Ismagilov, *Chem. Soc. Rev.*, 2010, **39**, 974.
31 D. Pekin, Y. Skhiri, J. C. Baret, D. Le Corre, L. Mazutis, C. Ben Salem, F. Millot, A. El Harrak, J. B. Hutchison, J. W. Larson, D. R. Link, P. Laurent-Puig, A. D. Griffiths and V. Taly, *Lab Chip*, 2011, **11**, 2156.
32 S. L. Angione, A. Chauhan and A. Tripathi, *Anal. Chem.*, 2012, **84**, 2654.
33 Y. Zhang, S. Park, K. Liu, J. Tsuan, S. Yang and T. H. Wang, *Lab Chip*, 2011, **11**, 398.
34 V. Srinivasan, V. K. Pamula and R. B. Fair, *Lab Chip*, 2004, **4**, 310.

